Scientia Iranica B (2012) 19 (5), 1346–1353

Sharif University of Technology

Scientia Iranica

Transactions B: Mechanical Engineering

www.sciencedirect.com

Research note

Control of an atomic force microscopy probe during nano-manipulation via the sliding mode method

M.H. Korayem [a,*], **M. Noroozi** [b,1], **Kh. Daeinabi** [b]

[a] *Department of Mechanical Engineering, Center of Excellence in Experimental Solid Mechanics and Dynamics, Iran University of Science and Technology, Tehran, P.O. Box 13114-16846, Iran*

[b] *Department of Mechatronics Engineering, Science and Research Branch, Islamic Azad University, Tehran, P.O. Box 14737-87996, Iran*

Received 2 March 2012; revised 12 May 2012; accepted 19 June 2012

KEYWORDS
AFM;
Chattering;
Lyapunov-based stability;
Nano-manipulation;
Sliding mode control.

Abstract Nowadays, designing a reliable controller for an Atomic Force Microscope (AFM) during the manipulation process is a main issue, since the tip can jump over the target nanoparticle and, thus, the process can fail. This study aims to design a Sliding Mode Controller (SMC) as a robust chattering-free controller to push nano-particles on the substrate. The first control purpose is positioning the micro cantilever tip at a desired trajectory by the control input force, which can be exerted on the micro cantilever in the Y direction by an actuator located at its base. The second control target is the micro-positioning stage in X, Y directions. The simulation results indicate that not only are the proposed controllers robust to external disturbances and nonlinearities, such as deflection of the AFM tip, but are chattering free SMC laws that are able to make the desired variable state to track a specified trajectory during a nano-scale manipulation.

1. Introduction

Nano-particle manipulation using AFM has created widespread interest over the last few years [1]. In addition, nano-manipulation is a first and critical step for achieving any complex functional nano-device, and its application can also be found in several fields, such as for nano-tribological characterization purposes [2–5]. Thus, some research has been developed to model AFM-based nano-manipulation [1,6,7]. Babahosseini et al. [8] presented a comprehensive and practical model of AFM tip-based nano-manipulation; the proposed model encompasses all effective physical and mechanical phenomena at the nano-scale. This model was also simulated for two prevalent friction models. Korayem and Zakeri [9], using a graphical method, researched the effects of existing parameters in the process of nano-particle pushing on the force and time required for manipulation. Daeinabi and Korayem [10] compared the applied load, adhesion force, contact radius and indentation depth of nano-particles for eight different nano-contact models. The dynamic behavior of a nano-particle during AFM-based pushing is studied in Refs. [11–13]. Using AFM as a nano-robot enables us to locate nano-particles in a desired position for micro/nano assembly in a two dimensional space to build miniaturized structures [14]. The manipulation process should be automated with less human intervention. Also, the need for designing a precise controller that guarantees a stable and accurate nano-manipulation task is obvious. Until now, some control schemes have been designed to make the AFM tip track a certain trajectory for the manipulation task. Hence, Yang and Jagannathan [15] proposed a NN-based controller, where the unknown part of the system dynamics is approximated by using a one-layer NN with an additional force control loop, guaranteeing the applied force to be close to the desired value. Delnavaz et al. [16] proposed a combined classical and second order sliding mode to the vibration control of the AFM tip in nano-manipulation tasks, but their nano-manipulation model was

* Corresponding author. Tel.: +98 21 77240540 50, +98 21 73912904; fax: +98 21 77240488.
E-mail addresses: Hkorayem@iust.ac.ir (M.H. Korayem), M_noroozi64@yahoo.com (M. Noroozi), kh_daeinabi@ieee.org (Kh. Daeinabi).
1 Tel.: +98 21 44480643.

Peer review under responsibility of Sharif University of Technology.

Production and hosting by Elsevier

doi:10.1016/j.scient.2012.06.026

Nomenclature

L	Microcantilever beam length
w	Microcantilever beam width
t	Microcantilever beam thickness
H	Tip height
E	Young's modulus
G	Shear modulus
ν	Microcantilever beam Poisson ratio
ρ	Density
ρ_p	Particle density
R_P	Particle radius
R_t	Tip radius
ψ	Pushing force angle
θ	Torsion angle of cantilever
K_θ	Stiffness coefficient of torsional spring
K_Y	Stiffness coefficient of linear spring
K_Z	Stiffness coefficient of linear spring
I_t	AFM tip inertia momentum
m_t	Tip mass
τ_s	Shear strength
ν_t	Tip Poisson ratio
ν_P	Particle Poisson ratio
ν_S	Substrate Poisson ratio
E_t	Tip Young modulus
E_P	Particle Young modulus
E_S	Substrate Young modulus
K	Modulus of elasticity of the material in contact
a	Contact radius
δ	Indentation depth
γ_t	Tip surface energy
γ_P	Particle surface energy
γ_S	Substrate surface energy
a_0	Interatomic separation distance
H_{tp}	Hamacker constant (tip-particle)
H_{ps}	Hamacker constant (particle-substrate)
ω	Surface energy between the nanoparticle and the tip/substrate
μ_S	Static coefficient of friction
μ_d	Dynamic coefficient of friction
F_Z	Normal tip force
F_Y	Lateral tip force
F_y, F_z	Spring forces (Cantilever bending forces)
M_θ	Moment
f_t, f_s	Tip-particle and particle-substrate friction
h_{set}	Desired tip center height
D_{set}	Initial horizontal distance of the tip/particle centers
V_{stage}	Stage velocity
V_{sub}	Substrate velocity
z_0	Normal deflection offset
w	Resonant frequency
Q	Amplification factor
e	Error
s	Sliding surface
V	Lyapunov function
D	Disturbance

simple. Furthermore, El Raifi and Youcef-Toumi [17] designed a robust adaptive controller for AFM tip positioning. Although various controllers are available to control the AFM probe as a nonlinear system, the sliding mode approach is proposed in this paper, which displays a satisfactory performance with a simple control structure and which is robust to model imprecision. During manipulation, the tip/particle/substrate system experiences complicated dynamics, and a perfect model of nano-manipulation is useful for successful control. The proposed modeling includes the coupled dynamics of the micro-cantilever and piezo tube actuator. Uncertainties due to the probe/sample contact are considered in the modeling.

The organization of the article is as follows: In Section 2, nano-manipulation and its nonlinear mathematical model are described. Then, in Section 3, the sliding mode control for the AFM-tip is designed and simulation results are provided. In Section 4, the dynamics of the AFM-surface is proposed, and in Section 5, the simulation results are demonstrated. Finally, the conclusion is presented in Section 6.

2. Nano-manipulation model

The AFM system used as a manipulation tool in this paper consists of a micro-cantilever beam with a sharp conical tip. The micro-cantilever is mounted on a piezoelectric actuator with a position sensitive photo detector, which receives a laser beam reflected from the end point of the beam to provide micro-cantilever deflection feedback [8]. The AFM tip moves and pushes the targeted particle on the immobile substrate, which is modeled as one torsional and two linear springs.

$$K_Z = \frac{Ewt^3}{4L^3}, \tag{1}$$

$$K_y = \frac{EW^3t}{4L^3}, \tag{2}$$

$$K_\theta = K_y^{\text{torsion}} H^2 = \frac{Gwt^3}{3L} = \frac{Ewt^3}{6L(1+\nu)}. \tag{3}$$

AFM geometry and material property are Young's modulus, E, shear modulus, G, length, L, width, W, and thickness, t.

Normal force, F_z, lateral force, F_y, and moment, M_θ, of the springs are proportional to the deflection and torsion of the micro-cantilever.

$$F_z = K_z z_c, \tag{4}$$

$$F_y = K_y y_c, \tag{5}$$

$$M_\theta = K_\theta \theta. \tag{6}$$

Figure 1 depicts a free body diagram of the AFM lumped-parameters model, where the spring force, moment, (F_z, F_y, M_θ) and interaction nanoscale force between the tip/particle $F_{tp}(t)$ are external forces exerted on the tip.

The local coordinates are set up at c and t, which correspond to the center of the micro-cantilever cross area and the center of the spherical tip apex. y_t and y_c are the tip base and the tip apex lateral movements, z_t and z_c are the tip base and tip apex vertical movements, ψ is pushing force angle and θ is the tip torsional angle about the x axis.

$$\ddot{\theta} = \frac{1}{(I_t + I_c)}(F_{tp}\cos\psi \acute{H}\sin\theta - k_\theta\theta + F_{tp}\sin\psi\acute{H}\cos\theta), \tag{7}$$

$$\ddot{y}_t = \frac{1}{(m_t + m_c)}\left(-F_{tp}\sin\psi - k_y(y_t + \acute{H}\sin\theta) - (\ddot{\theta}\acute{H}\cos\theta - \acute{H}\dot{\theta}^2\sin\theta)\left(\frac{m_t + 2m_c}{2}\right)\right), \tag{8}$$

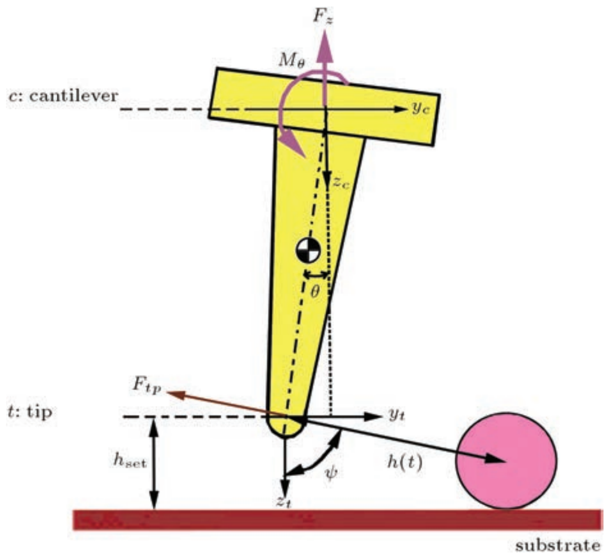

Figure 1: Free body diagram of AFM lumped parameters model during nano-manipulation [8].

$$\ddot{z}_t = \frac{1}{(m_t+m_c)}\left(-F_{\text{tp}}\cos\psi - k_z(z_t - \acute{H}\cos\theta) - \left(\frac{m_t+2m_c}{2}\right)(\ddot{\theta}\acute{H}\sin\theta + \acute{H}\dot{\theta}^2\cos\theta)\right), \qquad (9)$$

where I_t and I_c are the inertia momentums of the AFM tip and microcantilever, and c, m_t and m_c are their masses, respectively. H is the tip height and ($\acute{H} = H + \frac{t}{2}$). F_{tp} is Derjaguin interaction force defined as:

$$F_{\text{tp}}(h(t)) = \begin{cases} -\dfrac{\bar{H}_{\text{tp}}\tilde{R}}{6h(t)^2} & \text{if } a_0 < h(t) \le 100\text{ nm} \\ -\dfrac{\bar{H}_{\text{tp}}\tilde{R}}{6a_0^2} + \dfrac{4}{3}K_{\text{tp}}\sqrt{\tilde{R}}(a_0 - h(t))^{3/2} & \text{if } h(t) \le a_0, \end{cases} \qquad (10)$$

$$K_{\text{tp}} = \left[\frac{(1-\nu_t)^2}{E_t} + \frac{(1-\nu_p)^2}{E_p}\right]^{-1}, \qquad (11)$$

$$\tilde{R} = R_t R_p/(R_t + R_p), \qquad (12)$$

where $\bar{H}_{\text{tp}}$ is the Hamacker constant, a_0 is the interatomic separation distance introduced to avoid numerical divergence of F_{tp}, K_{tp} is the effective tip/particle elastic modulus, E_t and E_p are the Young's modulus of the tip and particle, respectively, and ν_t and ν_p are the Poisson coefficient of the tip and particle. $\tilde{R}$ is the effective tip/particle radius. The time-varying separation distance between the tip/particle is $h(t)$. Also, ψ, the angle of F_{tp}, is defined as [8]:

$$h(t) = \sqrt{(D_{\text{set}} - y_t + y_p)^2 + (h_{\text{set}} - R_P + \delta_{\text{ps}})^2} + \delta_{\text{tp}} - (R_t + R_p), \qquad (13)$$

$$\psi = \tan^{-1}\left(\frac{D_{\text{set}} - y_t + y_p}{h_{\text{set}} - R_P + \delta_{\text{ps}}}\right), \qquad (14)$$

where y_p is the total lateral movement of the particle on the substrate in the y-axis. D_{set} is the initial horizontal distance between the tip and particle centers, and h_{set} is the tip center height. R_t is the radius of the spherical tip apex and R_p is the ball-like particle radius (R_p assumes 150 nm [8]). $\delta_{\text{ps}}, \delta_{\text{tp}}$ are nanoscale penetration depths on the particle/substrate and tip/particle contact surfaces [10].

Table 1: System parameter values [1,8,16].

Unit	Value	Symbol
L	$225 * 10^{-6}$	m
w	$48 * 10^{-6}$	m
t	$1 * 10^{-6}$	m
H	$12 * 10^{-6}$	m
E	$169 * 10^{9}$	Pa
G	$66.54 * 10^{9}$	Pa
R_P	$150 * 10^{-9}$	m
R_t	$25 * 10^{-9}$	m
I_t	$23.4 * 10^{-22}$	kg·m^2
m_t	$3 * 10^{-10}$	kg
ρ	2330	kg/m^3
a_0	$3.75 * 10^{-10}$	m
$H_t p$	$33.6 * 10^{-20}$	J
H_{ps}	$8.1 * 10^{-20}$	J
μ_S	0.5	None
μ_d	0.4	None
τ_s	$19 * 10^{6}$	Pa

In Figure 1, nano-particle dynamics and forces are considered and shown, when the particle is pushed by the AFM tip [1].

The motion equation of the nano-particle in the y direction can be written as follows:

$$\ddot{y}_p = \frac{1}{m_p}(F_{\text{tp}}\sin\psi - \text{sign}(\dot{y}_p)F_{\text{frict}}), \qquad (15)$$

where $\ddot{y}_p(t)$ is the nanoparticle acceleration, $F_{\text{tp}}\sin\psi$ is the tip/particle lateral interaction force, which we nominate as the pushing force, and F_{frict} is the nanoscale friction force on the contact surface of the particle/substrate. The AFM mechanical properties and geometric constants are demonstrated in Table 1.

Figure 2 demonstrates the frictional force and the lateral AFM tip force on the particle (or pushing force). Both graphs increase and fluctuate harmonically around a fixed value. During an oscillation, the amplitude of the pushing force is greater than the friction force above a wave, but friction force is greater below the wave. This difference leads to alternative positive and negative particle acceleration during the nano-manipulation. Also, Figure 2 shows that the nano-particle stays at the initial position until time 13 μs, and, then, the particle begins to slide on the substrate. The average velocity of the nano-particle is about 0.5 μm/s, which is equal to the velocity of the probe stage as in [8].

3. Design controller

In this section, design of a sliding mode controller [18] as a robust chattering-free control in contact-mode, to control the AFM tip during the nano-manipulation process, for accomplishment of an effective nano-manipulation task, is studied, in order to achieve the main goal of a full automatic nano-manipulation system without direct intervention of an operator. The major aim is to control and position the micro-cantilever tip at a desired trajectory, especially at a constant tip angle and displacement during lateral nano-manipulation by the control input force. The nonlinear system of concern is represented by:

$$\ddot{y} = f(Y) + g(Y)U, \qquad (16)$$

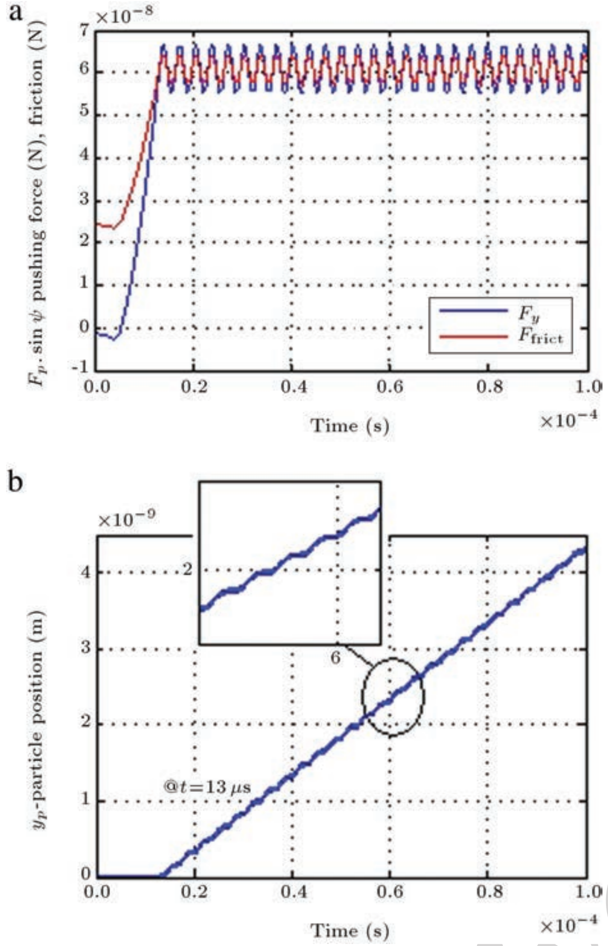

Figure 2: (a) Pushing and friction forces. (b) Tip and particle position [8].

where $f(Y)$ and $g(Y)$ are nonlinear functions. The number of state variables are eight, they are θ, y_t, y_p, z_t and their derivatives, and U is a control input.

$$\frac{dy_1}{dt} = \dot{\theta} = y_5,$$
$$\frac{dy_2}{dt} = \dot{y}_t = y_6,$$
$$\frac{dy_3}{dt} = \dot{y}_p = y_7,$$
$$\frac{dy_4}{dt} = \dot{z}_t = y_8,$$
$$\frac{dy_5}{dt} = \ddot{\theta} = \frac{1}{(I_t + I_c)}(F_{tp}\cos\psi \acute{H}\sin y_1 + F_{tp}\sin\psi \acute{H}\cos y_1 - k_\theta y_1 + U),$$
$$\frac{dy_6}{dt} = \ddot{y}_t = \frac{1}{(m_t + m_c)}\left(-F_{tp}\sin\psi - k_y(y_2 + \acute{H}\sin y_1) - \left(\frac{dy_5}{dt}\acute{H}\cos y_1 - \acute{H}\dot{y}_1^2\sin y_1\right)\left(\frac{m_t + 2m_c}{2}\right)\right),$$
$$\frac{dy_7}{dt} = \ddot{y}_p = \frac{1}{m_p}(F_{tp}\sin\psi - \mathrm{sign}(\dot{y}_p)F_{frict}),$$

Table 2: Values of the controller used in simulation.

Parameter	Value	Parameter	Value
λ_1	1e+8	φ	1e−5
λ_2	1e−1	K	1.8e+7
λ_3	9e+9	–	–

$$\frac{dy_8}{dt} = \ddot{z}_t = \frac{1}{(m_t + m_c)}\left(-F_{tp}\cos\psi - k_z(z_t - \acute{H}\cos y_1) - \left(\frac{m_t + 2m_c}{2}\right)\left(\frac{dy_5}{dt}\acute{H}\sin y_1 - \acute{H}\dot{y}_1^2\cos y_1\right)\right). \quad (17)$$

The algorithm of control is shown in Figure 3.

Finding a proper sliding surface for such a system is not a routine task. The sliding surfaces of this system can be defined as:

$$e_1 = \theta - \theta_{set}, \quad (18)$$
$$e_2 = y_t - y_{t\cdot set}, \quad (19)$$
$$s_1 = \dot{\theta} + \lambda_1 e_1, \quad (20)$$
$$s_2 = \dot{y}_t + \lambda_3 e_2. \quad (21)$$

In Eqs. (18) and (19), e_1 and e_2 are errors, and $\lambda_1, \lambda_2 > 0$ are chosen to guarantee that e tends to zero. To have a stable system with the guarantee of stability of the feedback system, here the Lyapunov function is considered as follows:

$$V = |s_1| + \lambda_2 |s_2|. \quad (22)$$

Here, λ_2 is a positive variable defined real number between 0 and 1, hence, $V \geq 0$. In Table 2, the values of controller parameters are presented.

$$\dot{V} = \mathrm{sign}(V). \quad (23)$$

The derivative of Eq. (22) is given by:

$$\dot{V} = \frac{s_1\dot{s}_1}{|s_1|} + \lambda_2\frac{s_2\dot{s}_2}{|s_2|} = \mathrm{sgn}(s_1)\dot{s}_1 + \lambda_2\mathrm{sgn}(s_2)\dot{s}_2. \quad (24)$$

Taking

$$\dot{s}_1 = \dot{y}_5 + \lambda_1\dot{e}_1 = f_1(y) + g_1(y)U + \lambda_1 y_5,$$

and

$$\dot{s}_2 = \dot{y}_6 + \lambda_3\dot{e}_2 = f_2(y) + g_2(y)U + \lambda_3 y_6,$$

U is presented by Eq. (25).

For improving the control behavior of AFM tip angle and displacement, and reducing the chattering phenomenon, a saturation function is proposed instead of a sign function ($\dot{V} = -\eta\,\mathrm{sat}(\frac{V}{\varphi})$). First, the sign function and, second, the saturation function (sat), are used. This function greatly reduces chattering as shown in Figure 4. The control objective is to choose U to make θ and y_t track θ_{set} and $y_{t\cdot set}$, respectively. Using Lyapunov-based stability, control signal U as a force input control, is presented as Eq. (25), given in Box I: where f_1, f_2 and g_1, g_2 are nonlinear functions in Eq. (16) for two different sliding surfaces (s_1, s_2). In Figure 4, the proposed sliding mode controller is shown in the presence of the disturbance that leads the tip angle, which is one of the nonlinearities caused by manipulation force on the desired trajectory. Also, the tip and micro-cantilever move together with the same velocity during nano-manipulation, and as a result the tip cannot jump over the target nano-particle and the process will be continued until the end.

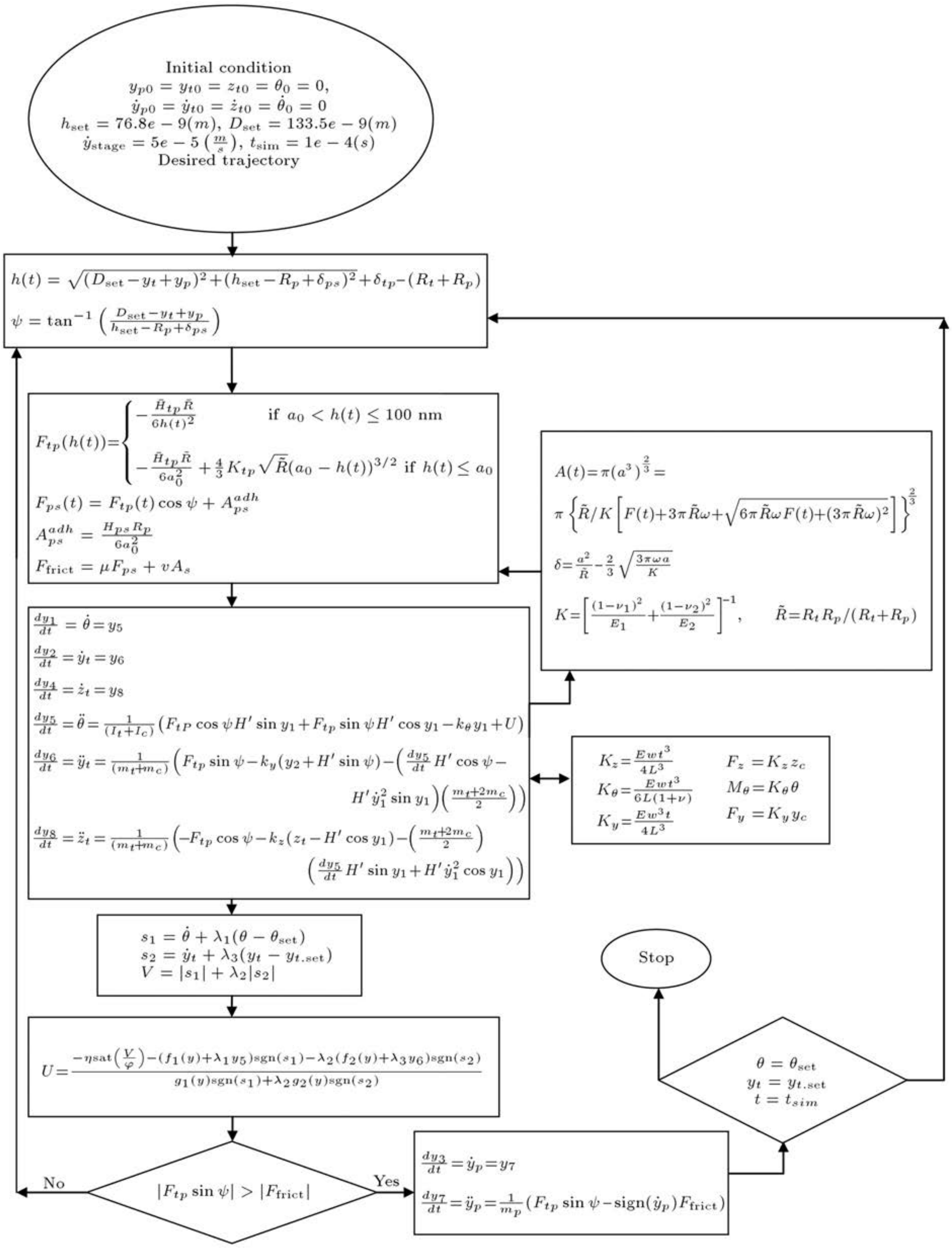

Figure 3: Algorithm of control nano-manipulation.

4. Dynamic of surface model

For atomic resolution positioning, piezoelectric actuators are utilized in the AFM system. By denoting the sample position on x, y, and z directions as x_s, y_s, and z_s, respectively, the dynamics of the stage along each axis are given as [15]:

$$\frac{1}{w_x^2}\ddot{x}_s + \frac{1}{w_xQ_x}\dot{x}_s + x_s + f_{\text{ps}}(z_s, z_{\text{sub}})\cos\gamma = \tau_x, \tag{26}$$

$$U = \frac{-\eta \mathrm{sat}\left(\frac{v}{\varphi}\right) - (f_1(y) + \lambda_1 y_5)\mathrm{sgn}(s_1) - \lambda_2 (f_2(y) + \lambda_3 y_6)\mathrm{sgn}(s_2)}{g_1(y)\mathrm{sgn}(s_1) + \lambda_2 g_2(y)\mathrm{sgn}(s_2)}, \quad (25)$$

Box I:

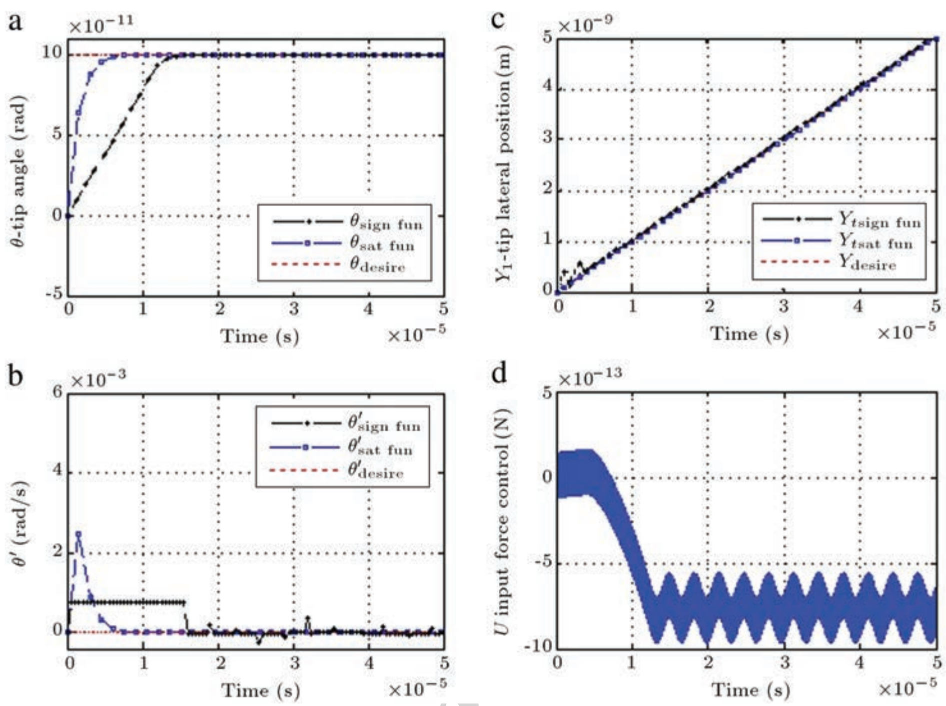

Figure 4: The SMC control of AFM tip (a) angle, (b) angle derivation, (c) displacement during nano-manipulation process, (d) input force control.

$$\frac{1}{w_y^2}\ddot{y}_s + \frac{1}{w_y Q_y}\dot{y}_s + y_s + f_{\mathrm{ps}}(z_s, z_{\mathrm{sub}}) \sin\gamma = \tau_y, \quad (27)$$

$$\frac{1}{w_z^2}\ddot{z}_s + \frac{1}{w_z Q_z}\dot{z}_s + z_s + F_{\mathrm{ps}}(z_s, z_{\mathrm{sub}}) \sin\gamma = \tau_z + A_{\mathrm{ps}}, \quad (28)$$

$$f_{\mathrm{ps}} = \mu_{\mathrm{ps}} F_{\mathrm{ps}}, \quad (29)$$

where $w, Q, f_{\mathrm{ps}}, \mu_{\mathrm{ps}}, F_{\mathrm{PS}}$ and τ are the resonant frequency, amplification factor, frictional force, particle-substrate sliding friction coefficient, particle-substrate interaction force and stage driving forces, respectively. A force controller will be designed such that it will change the horizontal position, x_s, y_s, of the stage from A to B, while z_s is at a desired value and constant. This will ensure that the tip contacts the particle with almost the same height away from the substrate during the pushing, while minimizing the chance of losing contact with the particle. This requirement also guarantees that a proper force will be applied to the sample without damaging it. The main control aim is to design a control input that guarantees a desired stage motion during nano-manipulation in X, Y directions.

5. Design controller for stage

At first, a sliding mode controller for the motion of the nano-particle from the (0, 0) point to the (0.5 μm, 0.5 μm) position is designed and compared with previous work [4,19], as observed in Figure 5.

$$e_s = \begin{bmatrix} x_s \\ y_s \end{bmatrix} - \begin{bmatrix} x_d \\ y_d \end{bmatrix}, \quad (30)$$

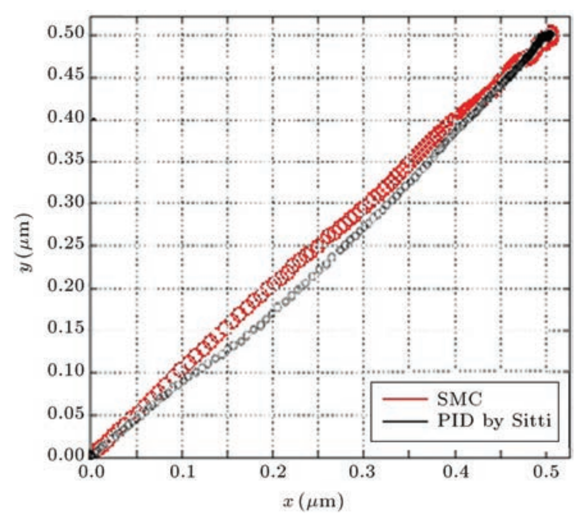

Figure 5: Comparison control motion of nano-particle during pushing from the (0, 0) point to (0.5 μm, 0.5 μm) position.

$$\begin{bmatrix} s_x \\ s_y \end{bmatrix} = \dot{e}_s - \begin{bmatrix} \lambda_1 & \lambda_2 \end{bmatrix} e_s, \quad (31)$$

$$\begin{bmatrix} \tau_x \\ \tau_y \end{bmatrix} = \left(\begin{bmatrix} -k_1 \mathrm{sat}(s_x) \\ -k_2 \mathrm{sat}(s_y) \end{bmatrix} - \begin{bmatrix} \lambda_1 & \lambda_2 \end{bmatrix} \begin{bmatrix} \dot{x}_s - \dot{x}_d \\ \dot{y}_s - \dot{y}_d \end{bmatrix} + \begin{bmatrix} \ddot{x}_d \\ \ddot{y}_d \end{bmatrix} - f - D \right) \Big/ g, \quad (32)$$

Table 3: Values of the controller used in simulation.

Parameter	Value	Parameter	Value
λ	1e+7	T	4.213e−5
φ	1e−10	A	25e−9
K	2e−13	α	7e−7

where $\begin{bmatrix} x_s & y_s \end{bmatrix}^T$, $\begin{bmatrix} x_d & y_d \end{bmatrix}^T$ and $\begin{bmatrix} \tau_x & \tau_y \end{bmatrix}^T$ present the system state, the desired trajectory for the stage and control input vector, respectively. $f = \begin{bmatrix} f_1 \\ f_2 \end{bmatrix}$ and $g \begin{bmatrix} g_1 \\ g_2 \end{bmatrix}$ are nonlinear functions in Eq. (16) for Eqs. (26) and (27). The disturbance is denoted as:

$$D = -\alpha + 2\alpha^{*}\text{rand}. \tag{33}$$

Comparison of the efficiency of the two controllers applied to AFM-stage system dynamics has shown successful trends in controlling the output of the nonlinear AFM-stage system. The striking feature of the sliding mode control is its robustness, with respect to f and g. We only need to know the upper bound during the sliding phase; the motion is completely independent of f and g. Also, the output signal achieves good tracking of the desired reference signal with a better settling time.

In this paper, a control strategy is proposed for the nonlinear AFM-stage system based on sliding mode approach, which is faced with external disturbances. This control algorithm is based on the Lyapunov technique, which is able to provide the stability of the system during tracking a circular path, with acceptable precision. The Lyapunov function is considered as follows [18]:

$$V = \frac{1}{2}s^2. \tag{34}$$

The sliding condition is defined by:

$$\frac{1}{2}\frac{d}{dt}s^2 \leq -\eta|s|. \tag{35}$$

The desired paths for x and y are:

$$x_d = (-A)\cos\left(\frac{t}{T}\right), \tag{36}$$

$$y_d = (-A)\cos\left(\frac{t}{T} + \pi/2\right). \tag{37}$$

The values of controllers used in the simulation are presented in Table 3. Simulation results indicate that the sliding mode controller that is proposed in order to control the AFM-stage and the particle within a predefined trajectory can achieve its objective with acceptable tracking accuracy (Figures 6 and 7).

6. Conclusion

Since the task of manipulating nano-objects is complex, due to the nonlinear cantilever and contact dynamics, a sliding mode controller, as a robust and reliable controller, has been presented for guiding the AFM tip and stage, so that the position of the nano-particle follows a predefined trajectory. First, positioning the micro-cantilever tip at a desired trajectory, especially at a constant tip angle and displacement, during lateral nano-manipulation, is controlled by the SMC method. Second, the micro-positioning stage, based on AFM nano-manipulation, is controlled by the SMC method in X and Y directions. The simulation results indicate that not only are the proposed controllers robust under external disturbance, but that they are also chattering free SMC laws, which are able to perform the pushing task successfully in term of tracking during nano-scale manipulation.

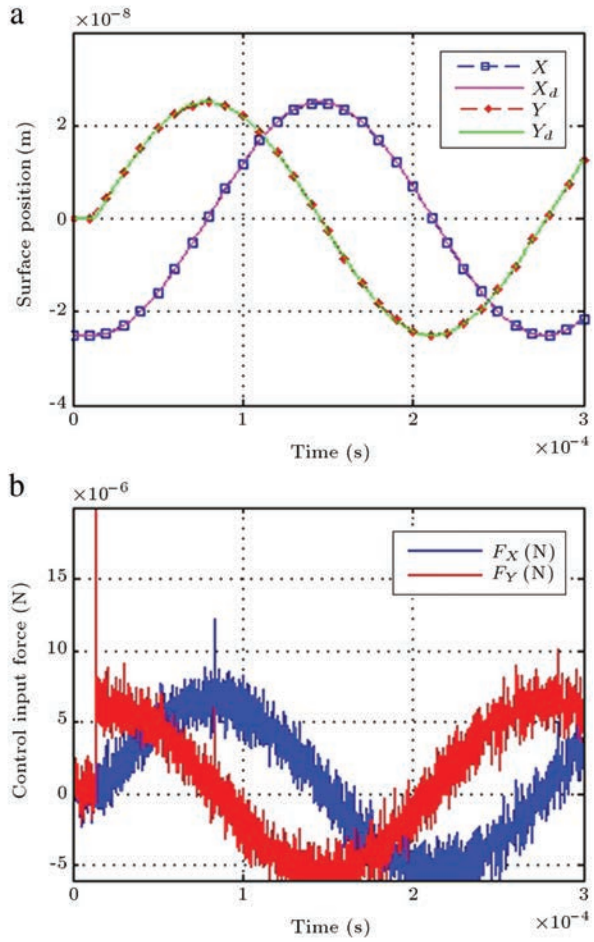

Figure 6: AFM-surface in presence of disturbance using SMC controller. (a) x and y surface positions, (b) control input forces.

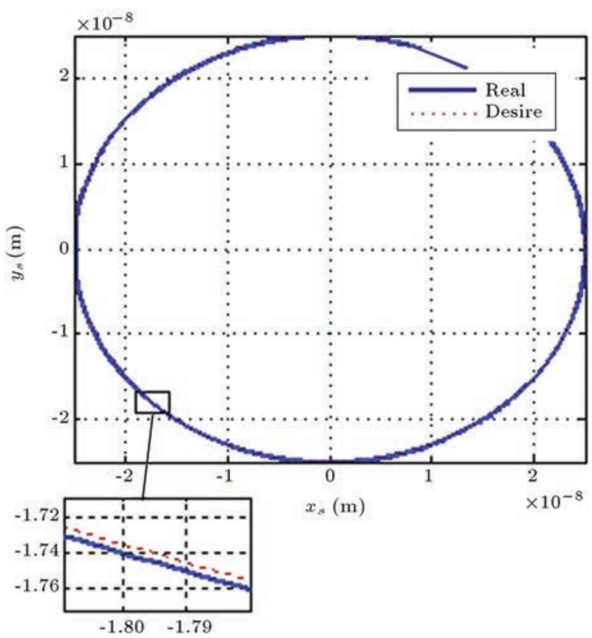

Figure 7: Input–output path using SMC controller.

References

[1] Tafazzoli, A. and Sitti, M. "Dynamic behavior and simulation of nanoparticle, sliding during nanoprobebased positioning", *Proc. of IMECE04, ASME International Mechanical Engineering Congress*, Anaheim, CA (2004).

[2] Sitti, M. "Atomic force microscope probe based controlled pushing for nano-tribological characterization", *IEEE/ASME Transactions on Mechatronics*, pp. 343–349 (2004).

[3] Sitti, M. and Hashimoto, H. "Teleoperated touch feedback from the surfaces at the nanoscale: modeling and experiments", *IEEE/ASME Transactions on Mechatronics*, pp. 1–12 (2003).

[4] Sitti, M. and Hashimoto, H. "Force controlled pushing of nanoparticles: modeling and experiments", *IEEE/ASME Transactions on Mechatronics*, pp. 199–211 (1999).

[5] Jalili, N. and Laxminarayana, K. "A review of atomic force microscopy imaging systems: application to molecular metrology and biological sciences", *Mechatronics*, pp. 907–945 (2004).

[6] Tafazzoli, A., Pawashe, C. and Sitti, M. "Atomic force microscope based two-dimensional assembly of micro/nanoparticles", *Proc. of IEEE Conf. on Nanotechnology* (2005).

[7] Tafazzoli, A. and Sitti, M. "Dynamic modes of nanoparticle motion during nanoprobe based manipulation", *ASME Proc. of 4th IEEE Conf. on Nanotechnology*, Munich, Germany (2004).

[8] Babahosseini, H., Mahboobi, S.H. and Meghdari, A. "Dynamic modeling and simulation of nanoparticle motion in AFM-based nanomanipulation using two nanoscale friction models", ASME/IMECE09 Florida, USA (2009).

[9] Korayem, M.H. and Zakeri, M. "Sensitivity analysis of nanoparticles pushing critical conditions in 2-D controlled nanomanipulation based on AFM", *International Journal of Advanced Manufacturing Technology*, 41, pp. 714–726 (2009).

[10] Daeinabi, Kh. and Korayem, M.H. "Indentation analysis of nano-particle using nano-contact mechanics models during nano-manipulation based on atomic force microscopy", *Journal of Nanoparticle Research*, pp. 1075–1091 (2010).

[11] Fathi, Y.M., Ghorbel, H. and Dabney, J.B. "Nanomanipulation modeling and simulation", *Proceedings of ASME International Mechanical Engineering Congress & Exposition*, November, Chicago, Illinois, USA (2006).

[12] Landolsi, F., Ghorbel, F.H. and Dabney, J.B. "An AFM-based nanomanipulation model describing the atomic two dimensional stick-slip behavior", *Proceedings of ASME International Mechanical Engineering Congress & Exposition*, Seattle, Washington, USA (2007).

[13] Jalili, N., Dadfarnia, M. and Dawson, D.M. "A fresh insight into the microcantilever-sample interaction problem in non-contact atomic force microscopy", *ASME Journal of Dynamic Systems, Measurement and Control*, 126, pp. 327–335 (2004).

[14] Sitti, M. and Hashimoto, H. "Two-dimensional fine particle positioning under optical microscope using a piezoresistive cantilever as a manipulator", *Journal of Micromechatronics*, pp. 25–48 (2000).

[15] Yang, Q. and Jagannathan, S. "Nanomanipulation using atomic force microscope with drift compensation", *Proceedings of the American Control Conference*, pp. 514–519 (2006).

[16] Delnavaz, A., Jalili, N. and Zohoor, H. "Vibration control of AFM tip for nano-manipulation using combined sliding mode approach", *Proceeding of 7th IEEE International Conference on Nanotechnology*, Hong Kong (2007).

[17] El Raifi, K., El Raifi, O. and Toumi, K.Y. "Modeling and control of AFM-based nano-manipulation systems", *Proceedings of the IEEE International Conference on Robotics and Automation*, pp. 157–162 (2005).

[18] Slotine, J.J. "Sliding controller design for nonlinear system", *International Journal of Control*, 40, pp. 421–434 (1984).

[19] Sitti, M. "Teleoperated 2-D micro/nano-manipulation using atomic force microscope", Ph.D. Thesis, University of Tokyo, Japan (1999).

Moharam Habibnejad Korayem was born in Tehran, Iran, in 1961. He received his B.S. (Hon) and M.S. degrees in Mechanical Engineering from Amirkabir University of Technology, Iran, in 1985 and 1987, respectively, and his Ph.D. degree in Mechanical Engineering from the University of Wollongong, Australia, in 1994. He is currently Professor of Mechanical Engineering at Iran University of Science and Technology, Iran, where, for the last 17 years, he has been involved in teaching and research activities in the area of robotics.

His research interests include dynamics of elastic mechanical manipulators, trajectory optimization, symbolic modelling, robotic multimedia software, mobile robots, industrial robotics standard, robot vision, soccer robot, and the analysis of mechanical manipulators with maximum load carrying capacity. He has published and presented more than 400 papers in international journals and at conferences in his area of expertise.

Marziye Noroozi was born in Iran, in 1986. She received her B.S. degree in Robotics Engineering from Shahrood University of Technology, in 2008, and her M.S. degree in Mechatronics Engineering from the Science and Research Branch of the Islamic Azad University, Tehran, in 2011.

Her research interests include robotics systems, micro/nano-mechatronics, industrial automation and mechatronics systems.

Khadijeh Daeinabi received her B.S. degree in Computer Engineering from Azad University, Central Tehran Branch, and her M.S. and Ph.D. degrees in Mechatronics Engineering from the Science and Research Branch of the Islamic Azad University, Tehran, Iran. She achieved first student rank in B.Sc. and M.Sc. levels. She has published and presented more than 8 papers in international journals and at conferences in Nano-Mechanics, Nano-Particle Manipulation and Atomic Force Microscopy. She is a Member of IEEE. Her research interests include nano-robotics systems, nano-mechatronics systems, nano-mechanics, industrial and intelligent robots.